Stretchable Organic Solar Cells

*Darren J. Lipomi, Benjamin C.-K. Tee, Michael Vosgueritchian, and Zhenan Bao**

The intrinsic flexibility of thin-film materials imparts mechanical resilience, enables convenient roll-to-roll processing,[1] and permits the fabrication of collapsible and portable devices.[2] Several of the most interesting and important potential applications of these materials, however, require elasticity under tensile strain ("stretchability") as well as flexibility.[3–5] Full mechanical compliance is a prerequisite for biocompatibility,[6,7] integration with textiles,[8] moving parts of machinery and internal organs,[9,10] and one-time bonding to curved surfaces such as the exteriors of buildings, automobiles, and lenses.[11] While the extremely creative recent work of Rogers[12] and Someya,[13–15] has demonstrated stretchable devices such as biological sensors,[10] photodetectors on hemispherical substrates,[16] and active-matrix displays,[15] stretchable sources of power have received less attention. In a recent demonstration, Bauer and coworkers produced a dry-cell battery by dispersing the components in an elastomeric matrix,[17] while Yu et al. reported a stretchable supercapacitor based on thick, buckled films of carbon nanotubes.[18] Primary, renewable sources of power, e.g., solar cells, for stretchable devices would advance the field further. This communication describes the use of mechanical buckling to produce the first intrinsically stretchable organic solar cell, which can accommodate strains of 27%, reversibly.

There are two common strategies used for imparting elasticity to materials that are intrinsically rigid. The first method is to disperse the conductive material in an intrinsically elastic matrix.[14,19] The second is to exploit the buckling instability that occurs when compressive strain is applied to a system comprising a rigid film on an elastomeric substrate.[20] When the substrate compresses, sinusoidal waves arise in the thin film whose pitch is related to the differences in mechanical properties of the thin film and the substrate, the thickness of the film, and the magnitude of the strain.[21] The early important work on this form of "physical self-assembly" was performed by Whitesides,[20,22] Wagner,[23,24] and Suo,[23] using evaporated metals on poly(dimethylsiloxane) (PDMS) substrates. The waves in buckled thin films convert tensile strains of the whole film to bending strains of the individual buckles within the film, and thus convert a film that is brittle upon tensile strain to one that is elastic. Rogers and coworkers, who used buckling to produce "wavy" single-crystalline silicon, produced high-performance microelectronic devices that can be repeatedly stretched,[3,25] bonded to hemispherical substrates,[16] or conformed to a mammalian heart[9] or brain.[10]

D. J. Lipomi, B. C.-K. Tee, M. Vosgueritchian, Prof. Z. Bao
Department of Chemical Engineering
Stanford University
381 North-South Mall, Stanford, CA, USA
E-mail: zbao@stanford.edu

DOI: 10.1002/adma.201004426

Using a procedure first described by Stafford et al.,[21] Khang and coworkers recently used buckling to determine the elastic moduli of materials of interest in organic electronics.[26] The authors applied small compressive strains (2%) to films of poly(3,4-ethylenedioxythiophene):poly(styren esulfonate) (PEDOT:PSS) and a blend of regioregular poly(3-hexylthiophene) (P3HT) and (6,6)-phenyl-C_{61}-butyric acid methyl ester (PCBM) on a PDMS support. The authors found buckles in the films whose micron-scale pitch increased with the value of the pre-strain and the thickness of the films, and decreased with the stiffness of the film. They determined values of elastic moduli for these materials (1.3 GPa for PEDOT:PSS and 6.2 GPa for P3HT:PCBM) that were similar to those reported in the literature using more direct, but less convenient, methods of metrology.[26] The authors did not, however, use these buckled films in devices.

Solar cells comprising organic semiconductors are potentially low-cost alternatives to devices made of crystalline and polycrystalline silicon and other thin-film materials.[27] In principle, the inferior performance and environmental stability of organic semiconductors can be offset by the low intrinsic cost of organic materials, the relaxed requirements of purity, the minute thicknesses of material required (≤100 nm), and the relative ease with which they can be processed from solution.

The strategy that encompasses most research on organic photovoltaics (OPV) is a combination of increasing the efficiency,[28] lowering the cost,[29] and prolonging the lifetime[30] of the devices. The hope is to achieve a lower amortized cost per peak watt with OPV than with other technologies. Another strategy is to focus on areas where OPV can "run away" with part of the market by exploiting characteristics of OPV that inorganic materials do not possess. For example, OPV devices can be bent, reversibly, into hairpin turns.[31] This extreme level of compliance suggests that they could also be made to be stretchable using the buckling phenomenon. The ability to stretch an OPV device reversibly could enable integration of solar energy with moving parts and curved surfaces other than cones and cylinders. Additionally, elastic solar cells would be more resistant to fracture under tensile and bending strain than non-stretchable devices, and might increase the lifetime of OPV devices against mechanical failure.[32]

The most well characterized system in the field of OPV comprises a blend of P3HT and PCBM, whose details are described elsewhere.[2,33,34] **Figure 1** summarizes the procedure we used to fabricate a device of these materials on a pre-strained substrate. The PDMS membrane was stretched, clamped to a glass substrate (step 1), and spin-coated with PEDOT:PSS, followed by P3HT:PCBM (step 2). We extruded drops (diameter ~ 3 mm) of eutectic gallium-indium (EGaIn; work function = 4.3 eV) from a syringe,[35] and placed them on the surface of the PEDOT:PSS/P3HT:PCBM film (step 3). We then removed the clips and separated the device from the glass (step 4). The device

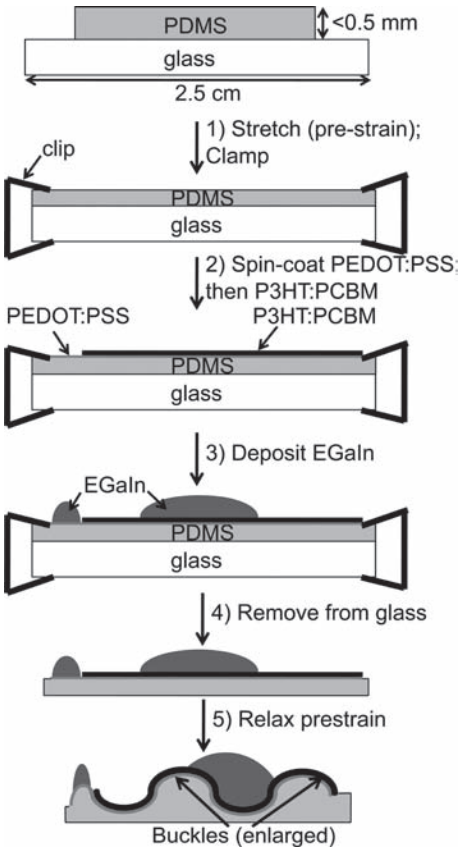

Figure 1. Summary of the procedures used to fabricate stretchable organic solar cells.

contracted spontaneously (step 5), and produced buckles in the PEDOT:PSS/P3HT:PCBM film. The EGaIn conformed to the microscopic buckles in the P3HT:PCBM film. We tried using the conventional top contact—evaporated aluminum—but it cracked catastrophically upon release of the pre-strain.

We chose to use PEDOT:PSS alone for the transparent, high-work-function electrode—as opposed to tin-doped indium oxide (ITO) or a combination of ITO and PEDOT:PSS—because ITO films are brittle, and we were concerned that they would crack upon release of the pre-strain. The drop of EGaIn, which we used as a top contact,[35] defined a circular device area, which compressed into an elliptical shape upon release of the pre-strain. We fastened copper wires to the device and placed the tips of the wires into the drops of EGaIn. In the ambient air, EGaIn is covered by a "skin" that consists of oxides of gallium.[36] The skin permitted drops of the liquid metal to retain their shapes when the substrate was tilted or even inverted.[37] EGaIn is unique among liquid metals because it can wet hydrophobic surfaces, and the oxide skin has the ability to hold onto metal wires such that they did not need to be repositioned when straining the devices.[36] We found that the sheet resistance (R_S = 750 Ω/sq with 96% transmittance) of a buckled, 100 nm, PEDOT:PSS film alone does not deteriorate at strains less than the pre-strain, and can be stretched at least 1000 times (the maximum number of stretches applied) before degradation in electronic performance (Figure S1, Supporting Information).

Figures 2a–f show films of P3HT:PCBM on PEDOT:PSS on a pre-strained PDMS substrate at six different stages in the strain-history of the films. The pre-strained (20%) film displayed no regular features (Figure 2a). The relaxed film exhibited buckles perpendicular to the axis of pre-strain, with a pitch of 10 μm (Figure 2b); re-stretching the film produced buckles parallel to the axis of pre-strain (Figure 2c); and relaxing the film a second time (Figure 2d) produced buckles with an appearance indistinguishable from Figure 2b. After stretching and relaxing the film 100 times, creases appeared parallel to the axis of the pre-strain (Figure 2e, inset). Stretching the film beyond the value of the pre-strain produced cracks in the film (Figure 2f). We attribute the features (buckles and creases) in the film that run parallel to the axis of strain upon stretching to and beyond the value of the pre-strain to the Poisson effect. The axis perpendicular to the pre-strain undergoes tensile strain upon relaxation and compressive strain upon stretching. We have not determined the mechanism by which the PEDOT:PSS/P3HT:PCBM film accommodates the tensile strain perpendicular to the pre-strain when fully relaxed and to what extent, if at all, the film delaminates from the PDMS substrate. The Supporting Information contains photographs of the apparatus used to pre-strain to the substrate, and to apply strain to the devices when tested for photovoltaic properties (Figure S2).

We first compared the photovoltaic properties of devices on different substrates and with different transparent electrodes. **Figure 3**a plots *J*–*V* characteristics of three un-optimized bulk heterojunction devices in the dark and illuminated with a flux of 100 mW/cm^2 simulating the AM 1.5G spectrum: a control device comprising a glass substrate and a transparent electrode comprising ITO and PEDOT:PSS ("ITO"), a control device without the ITO ("Glass"), and a device fabricated on a pre-strained PDMS membrane bearing a PEDOT:PSS film ("PDMS"). We used layers of PEDOT:PSS of 100 nm, P3HT:PCBM of 90 nm, identical annealing conditions, and EGaIn top electrodes for all devices. For each device, we measured the area of contact between the EGaIn and the P3HT:PCBM; most devices had areas of ~0.05 cm^2. The control device, "ITO", has the architecture most similar to the state-of-the art in the literature, with the notable substitution of EGaIn for evaporated aluminum. As expected, this architecture produced the most efficient device with the following figures of merit: short-circuit current density (J_{SC}) = 5.9 mA/cm^2; open-circuit voltage (V_{OC}) = 585 mV; fill factor (*FF*) = 0.58; and power conversion efficiency (*PCE*) = 2.0%. (This value of efficiency is lower than that of the best reported devices based on P3HT:PCBM. We attribute losses in efficiency primarily to the fact that we did not use electronic grade P3HT, which has higher purity and regioregularity than did the material we used.) The control device on glass without ITO produced lower values for all figures of merit (*PCE* = 0.50%), but the properties of the device on pre-strained PDMS were similar to those of the device on a glass substrate.

After determining that an organic solar cell fabricated on PDMS—without ITO—with a liquid EGaIn top contact was functional, the next step was to fabricate the same device on a pre-strained PDMS membrane, release the pre-strain, and measure the photovoltaic characteristics as a function of strain. Figure 3b plots current vs. voltage (*I*–*V*) of the photovoltaic response of a representative device with the architecture PDMS

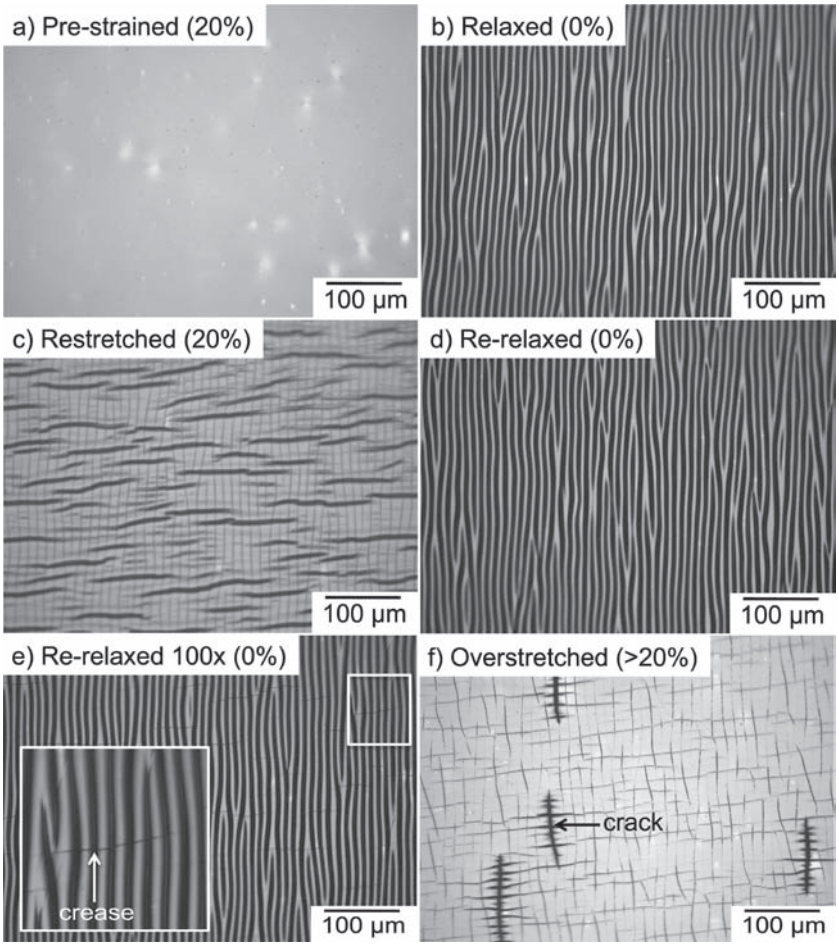

Figure 2. Optical images of PEDOT:PSS/P3HT:PCBM films on a pre-strained PDMS substrate.

(~0.5 mm)/PEDOT:PSS (120 nm)/P3HT:PCBM (90 nm)/EGaIn, and pre-strained 20%, under seven levels of strain, from 0 to 22.2%. The area of the device under 0% strain was 0.045 cm^2. At each level of strain past 0%, the device exhibited increases in short-circuit current (I_{SC}) and V_{OC}. (Note that we plotted current, not current density, to illustrate the change in the photovoltaic properties during the first application of strain.) The increase in the area of the device that occurred with strain cannot, by itself, account for the evolution of the *I*–*V* curves, because V_{oc} should be independent of area.

After the first full cycle of applied strain, the properties of the device remained approximately constant as a function of strain: I_{sc} scaled with the area of the device, and V_{oc} was independent. Figure 3c shows four plots of current density (that is, the current adjusted for the change in area) vs. voltage from the same device as shown in Figure 3b at 0% and 18.5% strain, after the second and eleventh full cycles of strain up to 18.5%. When stretched to 18.5% after eleven full cycles, the device exhibited the following figures of merit under a flux of 95 mW/cm^2: J_{SC} = 7.4 mA/cm^2; V_{OC} = 415 mV; fill factor (*FF*) = 0.38; and *PCE* = 1.2%. Stretching beyond 22.2% produced cracks in the active layer (visible by eye), and concomitant reductions in J_{SC}, *FF*, and *PCE* (Figure S3, Supporting Information). Devices pre-strained to 27% (the maximum pre-strain tested) could accommodate strains up to that amount, reversibly (Figure S4, Supporting Information). We did not determine the upper limit of the pre-strain, but it is, in principle, governed by the strain at failure of the elastic substrate, the flexural modulus of the active layer (flexibility accommodates buckles), and the adhesion of the active layer to the substrate. It was only practical, using our materials and methods, to impart and maintain initial pre-strains of 50% through all steps of fabrication. The devices did not return to their original lengths after fabrication and release of the pre-strain, however; the initial pre-strains of 50% produced effective pre-strains of 20%–30% after processing the PEDOT:PSS and P3HT:PCBM layers at elevated temperatures because of permanent stretching of the PDMS substrate that occurred when heated.

The observation that the photovoltaic characteristics were nearly independent of strain is remarkable, because stretching the device involves a complicated interplay of processes that could affect the photovoltaic properties in different ways. For example, stretching decreases the buckling amplitude and wavelength, which changes the optical path length through the PEDOT:PSS and the P3HT:PCBM and thus influences the absorption of light. The buckling also changes the geometry of the electric field within the device. Mechanical effects—stretching, bending and unbending of polymer chains—could influence the mechanism of charge transport in the materials. The fact that the photovoltaic properties are nearly independent of these disparate effects is somewhat serendipitous, because it would simplify integration of these devices with other components.

The buckling phenomenon provides a convenient platform on which to impart elasticity under tensile strain to organic electronic devices that are otherwise inelastic. The devices are, at present, not competitive with the state of the art in OPV devices in terms of efficiency, but we expect that an improved transparent electrode (perhaps the substitution of carbon nanotubes for ITO),[31] the use of a different conjugated polymer, antireflective coatings, and rigorous optimization would improve the devices. Two short-term goals are (1) to develop a stretchable conductor to replace the expensive EGaIn top electrode and (2) to produce devices with biaxial elasticity. Further work is also required to understand and possibly exploit the optical, geometrical, and mechanical effects of buckling. For example, buckling with controlled pitch could be an inexpensive way to increase the absorption of light by controlling the optical path of the incident flux.[38] Lessons learned could be applied to other photovoltaic systems, and might lead to more efficient, mechanically compliant, and ultimately more useful devices.

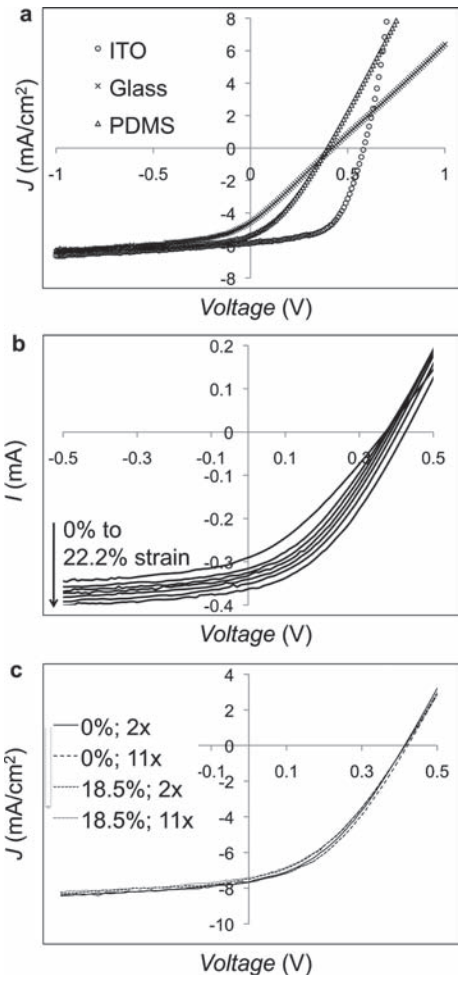

Figure 3. Photovoltaic properties of stretchable OPV devices.

Experimental Section

We began by puddle-casting a mixed and degassed poly(dimethylsiloxane) (PDMS) prepolymer (Dow Corning Sylgard 184, with a ratio of base to cross-linker of 10:1 by mass) against the polished surface of a silicon wafer. Curing at 60 °C for at least 2 h provided a PDMS membrane with a thickness of 200–500 μm. We cut the PDMS membrane into rectangles (3 cm × 1.5 cm) and placed them on glass slides (2.5 cm × 5 cm) with the side of the PDMS membrane that was cured against the silicon wafer facing up. We clipped one end with a binder clip, elongated the membrane by 50% with tweezers, and clipped the free end with a second binder clip. We chose the width of the glass slide of 5 cm such that the chuck of the spin-coater would sit in between the two binder clips. We pre-strained the membranes to 50% beyond their original lengths, but they did not return to their original lengths after fabricating the devices and releasing the pre-strain. Further cross-linking or plastic deformation of the PDMS when exposed to the heat (150 °C) required to anneal the PEDOT:PSS and P3HT:PCBM films produced smaller, "effective" pre-strains of 20%–30% when we finally removed clips. We reported this smaller value for all instances of the word "pre-strain" in this paper. We used sticky tape to clean the bottom surfaces of the PDMS membranes and the top surfaces of the glass slides to ensure conformal coverage of the glass slide with the PDMS. We removed the steel levers from the binder clips, cleaned the surfaces of the stretched PDMS membranes with tape, and activated the surfaces with UV/ozone for 20 min.

After activating the surfaces, we spin-coated the PDMS with PEDOT:PSS (H.C. Starck, Clevios PH1000, mixed with 5% dimethylsulfoxide, and 1% Zonyl FS-300 fluorosurfactant, obtained from Fluka) at 1000 rpm for 60 s, and then 2 krpm for 60 s. The Zonyl was necessary to promote wetting of the aqueous PEDOT:PSS suspension on the hydrophobic PDMS membranes. We annealed the PEDOT:PSS films on a hotplate at 150 °C for 30 min, turned off the hotplate, and allowed the substrates to cool for 30 min. It was necessary to place a small aluminum block between the binder clips on the underside of the substrate, between the binder clips, so that heat could be conducted efficiently from the surface of the hotplate to the glass. At a spin speed of 1000 rpm, the PEDOT:PSS films were 120 nm thick with R_S = 400 Ω/sq. After removing the substrates from the hotplate, we spin-coated them with 30 mg/mL total of a 1:1 solution of poly(3-hexylthiophene) (P3HT, regioregular, >90% head-to-tail regiospecificity, obtained from Aldrich, product of Rieke Metals) and [6,6]-phenyl C_{61} butyric acid methyl ester (PCBM, >99%, Aldrich) in *ortho*-dichlorobenzene (*o*-DCB) at 700 rpm for 1 min and 2 krpm for 1 min. We exposed a region of PEDOT:PSS by wiping away some of the P3HT:PCBM with a swab soaked with chloroform or tetrahydrofuran. We transferred the substrates to a nitrogen-filled glovebox and annealed the films on a hotplate at 150 °C for 30 min, turned off the hotplate, and allowed the substrates to cool for 30 min. We removed the substrates from the glovebox and applied drops of eutectic gallium-indium (EGaIn, Aldrich, ≥99.99%) to the P3HT:PCBM film by extruding EGaIn from a stainless steel syringe needle. It was helpful to separate the drops from the syringe needle using a wooden stick. We calculated the areas of the devices by measuring the circular or elliptical contact area of the EGaIn from the underside of the device using a ruler and a microscope. Most devices had areas of ~0.05 cm^2.

After placing the drops of EGaIn on the P3HT:PCBM film and the exposed region of the PEDOT:PSS, we attached copper wires to the drops of EGaIn, and secured the wires to the glass substrate, or to a purpose-built portable stage to impose strain, with electrical tape (see Supporting Information). The total time outside the glovebox after annealing the P3HT:PCBM films was ~20 min. We returned the devices to a glovebox and used a Newport solar simulator with a flux of 100 mW/cm^2 that approximated the solar spectrum under AM 1.5G conditions. We measured the current density vs. voltage in the dark and under illumination using a Keithley 2400 Sourcemeter and collected the data electronically using a custom LabView script.

We measured R_s of PEDOT:PSS films using a four-point probe method using four equally spaced, collinear probes connected to a Keithley 2400 Sourcemeter. We recorded optical micrographs of buckled films using a Leica DM4000M microscope under bright-field illumination. From these images, we divided the width of the image by the number of buckles to yield the average pitch of the buckles. We performed measurements of optical transmission (UV–vis) of PEDOT:PSS films using a Cary 6000i spetrophotometer, and measurements of thickness with a Veeco Dektak stylus profilometer.

Supporting Information

Supporting Information is available from the Wiley Online Library or from the author.

Acknowledgements

This work was partially supported by the Global Climate and Energy Project at Stanford University. D.J.L. was supported by a U.S. Intelligence Community Postdoctoral Fellowship. B. C-K. T. was supported by the Singapore National Science Scholarship from the Agency for Science Technology and Research (A*STAR). The authors acknowledge Randall

Stoltenberg for assistance acquiring measurements of film thickness, and Prof. John Rogers for helpful discussions.

Received: December 1, 2010
Published online: February 25, 2011

[1] F. C. Krebs, T. Tromholt, M. Jorgensen, *Nanoscale* **2010**, *2*, 873.
[2] Y. G. Sun, J. A. Rogers, *Adv. Mater.* **2007**, *19*, 1897.
[3] J. A. Rogers, T. Someya, Y. G. Huang, *Science* **2010**, *327*, 1603.
[4] A. J. Baca, J. H. Ahn, Y. G. Sun, M. A. Meitl, E. Menard, H. S. Kim, W. M. Choi, D. H. Kim, Y. Huang, J. A. Rogers, *Angew. Chem., Int. Ed.* **2008**, *47*, 5524.
[5] M. C. LeMieux, Z. N. Bao, *Nat. Nanotechnol.* **2008**, *3*, 585.
[6] T. Someya, *Nat. Mater.* **2010**, *9*, 879.
[7] R. H. Kim, D. H. Kim, J. L. Xiao, B. H. Kim, S. I. Park, B. Panilaitis, R. Ghaffari, J. M. Yao, M. Li, Z. J. Liu, V. Malyarchuk, D. G. Kim, A. P. Le, R. G. Nuzzo, D. L. Kaplan, F. G. Omenetto, Y. G. Huang, Z. Kang, J. A. Rogers, *Nat. Mater.* **2010**, *9*, 929.
[8] F. C. Krebs, M. Biancardo, B. Winther-Jensen, H. Spanggard, J. Alstrup, *Sol. Energy Mater. Sol. Cells* **2006**, *90*, 1058.
[9] J. Viventi, D. H. Kim, J. D. Moss, Y. S. Kim, J. A. Blanco, N. Annetta, A. Hicks, J. L. Xiao, Y. G. Huang, D. J. Callans, J. A. Rogers, B. Litt, *Sci. Transl. Med.* **2010**, *2*, 1.
[10] D. H. Kim, J. Viventi, J. J. Amsden, J. L. Xiao, L. Vigeland, Y. S. Kim, J. A. Blanco, B. Panilaitis, E. S. Frechette, D. Contreras, D. L. Kaplan, F. G. Omenetto, Y. G. Huang, K. C. Hwang, M. R. Zakin, B. Litt, J. A. Rogers, *Nat. Mater.* **2010**, *9*, 511.
[11] I. Jung, G. Shin, V. Malyarchuk, J. S. Ha, J. A. Rogers, *Appl. Phys. Lett.* **2010**, *96*, 021110.
[12] D. H. Kim, J. A. Rogers, *Adv. Mater.* **2008**, *20*, 4887.
[13] T. Sekitani, T. Someya, *Adv. Mater.* **2010**, *22*, 2228.
[14] T. Sekitani, Y. Noguchi, K. Hata, T. Fukushima, T. Aida, T. Someya, *Science* **2008**, *321*, 1468.
[15] T. Sekitani, H. Nakajima, H. Maeda, T. Fukushima, T. Aida, K. Hata, T. Someya, *Nat. Mater.* **2009**, *8*, 494.
[16] H. C. Ko, M. P. Stoykovich, J. Z. Song, V. Malyarchuk, W. M. Choi, C. J. Yu, J. B. Geddes, J. L. Xiao, S. D. Wang, Y. G. Huang, J. A. Rogers, *Nature* **2008**, *454*, 748.
[17] M. Kaltenbrunner, G. Kettlgruber, C. Siket, R. Schwodiauer, S. Bauer, *Adv. Mater.* **2010**, *22*, 2065.
[18] C. J. Yu, C. Masarapu, J. P. Rong, B. Q. Wei, H. Q. Jiang, *Adv. Mater.* **2009**, *21*, 4793.
[19] M. Kujawski, J. D. Pearse, F. Smela, *Carbon* **2010**, *48*, 2409.
[20] N. Bowden, S. Brittain, A. G. Evans, J. W. Hutchinson, G. M. Whitesides, *Nature* **1998**, *393*, 146.
[21] C. M. Stafford, C. Harrison, K. L. Beers, A. Karim, E. J. Amis, M. R. Vanlandingham, H. C. Kim, W. Volksen, R. D. Miller, E. E. Simonyi, *Nat. Mater.* **2004**, *3*, 545.
[22] N. Bowden, W. T. S. Huck, K. E. Paul, G. M. Whitesides, *Appl. Phys. Lett.* **1999**, *75*, 2557.
[23] J. Jones, S. P. Lacour, S. Wagner, Z. G. Suo, *J. Vac. Sci. Tech. A* **2004**, *22*, 1723.
[24] S. P. Lacour, S. Wagner, Z. Y. Huang, Z. Suo, *Appl. Phys. Lett.* **2003**, *82*, 2404.
[25] W. M. Choi, J. Z. Song, D. Y. Khang, H. Q. Jiang, Y. Y. Huang, J. A. Rogers, *Nano Lett.* **2007**, *7*, 1655.
[26] D. Tahk, H. H. Lee, D. Y. Khang, *Macromolecules* **2009**, *42*, 7079.
[27] B. C. Thompson, J. M. J. Fréchet, *Angew. Chem., Int. Ed.* **2008**, *47*, 58.
[28] J. Peet, A. J. Heeger, G. C. Bazan, *Acc. Chem. Res.* **2009**, *42*, 1700.
[29] S. I. Na, B. K. Yu, S. S. Kim, D. Vak, T. S. Kim, J. S. Yeo, D. Y. Kim, *Sol. Energy Mater. Sol. Cells* **2010**, *94*, 1333.
[30] M. Jorgensen, K. Norrman, F. C. Krebs, *Sol. Energy Mater. Sol. Cells* **2008**, *92*, 686.
[31] M. W. Rowell, M. A. Topinka, M. D. McGehee, H. J. Prall, G. Dennler, N. S. Sariciftci, L. B. Hu, G. Gruner, *Appl. Phys. Lett.* **2006**, *88*, 233506.
[32] F. C. Krebs, T. D. Nielsen, J. Fyenbo, M. Wadstrom, M. S. Pedersen, *Energy Environ. Sci.* **2010**, *3*, 512.
[33] S. Gunes, H. Neugebauer, N. S. Sariciftci, *Chem. Rev.* **2007**, *107*, 1324.
[34] G. Li, V. Shrotriya, J. S. Huang, Y. Yao, T. Moriarty, K. Emery, Y. Yang, *Nat. Mater.* **2005**, *4*, 864.
[35] A. Du Pasquier, S. Miller, M. Chhowalla, *Sol. Energy Mater. Sol. Cells* **2006**, *90*, 1828.
[36] M. D. Dickey, R. C. Chiechi, R. J. Larsen, E. A. Weiss, D. A. Weitz, G. M. Whitesides, *Adv. Funct. Mater.* **2008**, *18*, 1097.
[37] R. C. Chiechi, E. A. Weiss, M. D. Dickey, G. M. Whitesides, *Angew. Chem., Int. Ed.* **2008**, *47*, 142.
[38] S. I. Na, S. S. Kim, J. Jo, S. H. Oh, J. Kim, D. Y. Kim, *Adv. Funct. Mater.* **2008**, *18*, 3956.